Geochemistry, Geophysics, Geosystems®

RESEARCH ARTICLE
10.1029/2022GC010671

The Interface Between Magma and Earth's Atmosphere

J. Kuhn[1], N. Bobrowski[1,2], and U. Platt[1]

[1]Institut für Umweltphysik, Universität Heidelberg, Heidelberg, Germany, [2]Istituto Nazionale di Geofisica e Vulcanologica—Osservatorio Etneo, Catania, Italy

Abstract Volatiles released from magma can form bubbles and leave the magma body to eventually mix with atmospheric air. The composition of those volatiles, as derived from measurements made after their emission, is used to draw conclusions on processes in the Earth's interior or their influences on Earth's atmosphere. So far, the discussion of the influence of high-temperature mixing with atmospheric air (in particular oxygen) on the measured volcanic gas composition is almost exclusively based on thermodynamic equilibrium (TE) considerations. By modeling the combined effects of C-H-O-S reaction kinetics, turbulent mixing, and associated cooling during the first seconds after magmatic gas release into the atmosphere we show that the resulting gas compositions generally do not represent TE states, with individual species (e.g., CO, H_2, H_2S, OCS, SO_3, HO_2, H_2O_2) deviating by orders of magnitude from equilibrium levels. Besides revealing the chemical details of high-temperature emission processes, our results question common interpretations of volcanic gas studies, particularly affecting the present understanding of auto-catalytic conversion of volcanic halogen species in the atmosphere and redox state determination from volcanic plume gas measurements.

Plain Language Summary A major fraction of magmatic gas emissions are released into the atmosphere from open vents. The emission processes are characterized by fast turbulent mixing with atmospheric air (within seconds) and associated rapid cooling. Hardly anything is known about the chemical kinetics within this brief mixing and cooling period. We simulate the chemical kinetics during the first seconds of hot magmatic gases in the atmosphere and find severe deviation to common interpretations and central thermodynamic equilibrium assumptions prevailing in volcanic gas geochemistry.

Key Points:

- We model the chemical kinetics of high-temperature volcanic gas emissions within the first seconds of mixing with atmospheric air
- We identify key chemical processes within the magma-atmosphere interface and quantify influences on the volcanic plume composition
- Our results question common assumptions prevailing in volcanic gas geochemistry and refine interpretations of gas emissions from open vents

Supporting Information:

Supporting Information may be found in the online version of this article.

Correspondence to:

J. Kuhn,
jkuhn@iup.uni-heidelberg.de

Citation:

Kuhn, J., Bobrowski, N., & Platt, U. (2022). The interface between magma and Earth's atmosphere. *Geochemistry, Geophysics, Geosystems*, *23*, e2022GC010671. https://doi.org/10.1029/2022GC010671

Received 24 AUG 2022
Accepted 29 OCT 2022

Author Contributions:

Conceptualization: J. Kuhn
Funding acquisition: J. Kuhn, N. Bobrowski, U. Platt
Methodology: J. Kuhn
Software: J. Kuhn
Visualization: J. Kuhn
Writing – original draft: J. Kuhn
Writing – review & editing: N. Bobrowski, U. Platt

1. Introduction

Volcanic gases crucially influence Earth's atmosphere, on long time scales by gradually altering the atmospheric redox state (Gaillard et al., 2011; Kasting, 1993), as well as on short time scales when large amounts are emitted instantaneously during large eruptions (Robock, 2000). Volcanic gas measurements reveal information about Earth's interior, and the chemistry within the cooled and diluted volcanic plume. In that context, the interface between the magmatic gases and the atmosphere and its influence on the gas composition requires consideration. Interpretations of fumarole emissions, particularly those which have considerably cooled at the point of sampling, include a quantitative treatment of gas-rock and gas-fluid interactions. The analysis encompasses both, thermodynamic equilibrium (TE) relationships and the quantification of relative rates of equilibration (see e.g., Giggenbach, 1987, 1996; Henley and Fischer, 2021). In contrast to that, the interaction between magmatic gas and atmospheric air in high-temperature emission processes, for example, at open vents, is difficult to access experimentally and therefore remains poorly studied. Such high-temperature volcanic gases are commonly solely interpreted on the basis of TE relations. While this is likely to be valid for gas bubbles within the magma body, we show that—in contrast to usual assumptions (e.g., Gerlach and Nordlie, 1975; Martin et al., 2006; Moussallam et al., 2019)—TE is not suited to describe magmatic gases at the direct interface between magma and atmospheric air and afterward. TE requires the Gibbs free energy to be minimized prior to macroscopic changes of the system. By modeling the chemical kinetics and turbulent atmospheric mixing in the magma-atmosphere interface, we show that major chemical conversions, cooling, and mixing usually take place on comparable time scales. This leads to complex interactions of these processes ultimately determining the gas composition of the plume within the first fractions of a second after emission into the atmosphere. Then, the gas composition greatly deviates from both, the magmatic gas TE and the TE of the diluted plume and its interpretation requires considering chemical kinetics (i.e., reaction rates) and the dynamics of the system.

2. Hydroxyl Radicals in a High-Temperature Mixture of Water and Oxygen

Numerous approaches to modeling hot volcanic gases found considerable amounts of hydroxyl radicals (OH, up to tens of ppm for higher temperatures, e.g., Bobrowski et al., 2007; Gerlach, 2004; Martin et al., 2012; Roberts et al., 2014, 2019; von Glasow, 2010) and drew the attention to volcanic HO_X ($OH + HO_2$). However, these studies remain without a comprehensive assessment of its origin and impacts.

The OH radical is extremely reactive and substantially influences atmospheric processes even when present in amounts as small as 0.1 ppt (Crutzen, 1974; Levy, 1971). Generally, the abundance of OH as an intermediate species is linked to high rates of chemical conversion. For instance, large amounts of OH are present in combustion flames (Cattolica et al., 1982) and the oxyhydrogen gas explosion (Willbourn & Hinshelwood, 1946).

The following mechanism outlines the dynamics of a plausible OH formation process in volcanic gases, its strong dependence on mixing dynamics, and its impact on the plume's composition. Simplified, the emission of hot magmatic gases into the atmosphere, can be thought of as hot water vapor (the most abundant magmatic gas constituent, ca. 50 to >99%, see Gerlach, 2004; Symonds et al., 1994) rapidly mixing with O_2 (see Figure 1). Before leaving the magma body, magmatic gases are assumed to be in TE because of the high temperatures and considerable dwelling times of gas bubbles within magma (Giggenbach, 1996; Oppenheimer et al., 2018). Thus, within a hot gas bubble, a certain amount of OH and H is formed from water decomposition (Bonhoeffer and Reichardt, 1928; Gerlach, 2004, Figure 1c). Immediately after the emission of the hot gas from the magma, mixing with ambient air introduces O_2, which, together with the emitted OH and H, provides the initiation of chain branching mechanisms that lead to further enhanced OH levels.

$$O_{2(atm)} + H \rightarrow OH + O \quad (1)$$

$$H_2O_{(mag)} + O \rightarrow 2\,OH \quad (2)$$

$$R_{(mag)} + OH \rightarrow RO + H \quad (3)$$

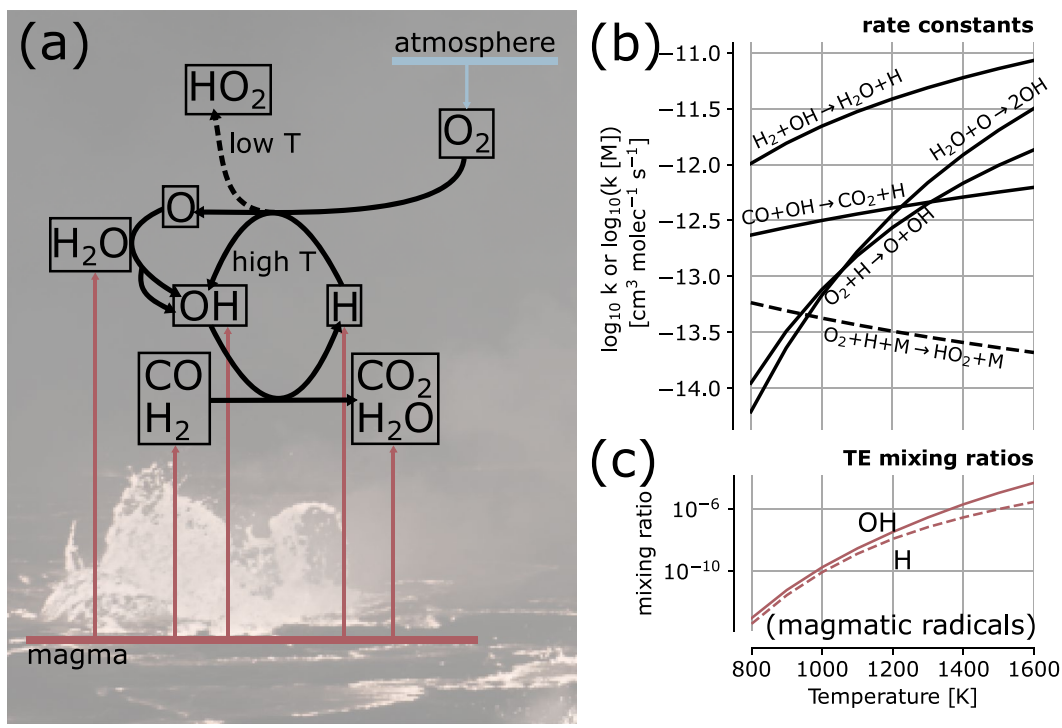

Figure 1. (a) Reaction scheme of an exemplary fast oxidation process when hot magmatic gases (in TE) mix with atmospheric O_2; (b) Respective reaction rate constants k as a function of temperature (pressure dependent reactions for 670 hPa, corresponding to a volcanic emission source at about 3,200 m above sea level); OH and H are formed from the decay of H_2O within magmatic gas bubbles and initiate the oxidation processes. (c) Shows the initial amounts of OH and H (in TE) as a function of emission temperature (670 hPa pressure).

This mechanism (rate constants in Figure 1b) oxidizes reduced plume components (e.g., H_2 or CO, denoted by R) in fast catalytic cycles. At the same time, mixing with atmospheric air causes rapid plume cooling, which slows down Reaction 2 and changes branching between Reaction 1 and HO_2 formation through (M denotes a neutral third molecule or atom, ensuring momentum conservation):

$$O_{2(atm)} + H + M \rightarrow HO_2 + M \quad (4)$$

This mechanism is only a small fraction of the kinetic processes studied in this work (see below). However, it already outlines the large extent to which the amount of OH (and other short-lived species) affects the chemical composition of volcanic gases with a strong dependence on mixing and cooling time scales. The widespread assumption that "the ambient air will simply quench and dilute the magmatic gas" (Gerlach & Nordlie, 1975; Martin et al., 2006) is therefore likely to be an oversimplification of a decisive process in the chemical evolution of volcanic gases in the atmosphere. The observations of flames occurring related to volcanic gas emissions (see e.g., Jaggar, 1917 and Figure S1 in Supporting Information S1) supports these considerations, though they may represent extreme examples of the processes examined here.

3. Rapid Atmospheric Mixing and Cooling of Magmatic Gas

We use a C-H-O-S kinetic chemical mechanism (Zeng et al., 2021, 52 species, 350 reactions, see also Figure S3 in Supporting Information S1) and model the first 10 s after the magmatic gas is emitted into the atmosphere. For each time instance the conversion rates of the plume constituents are calculated based on temperature-dependent rate constants of the individual chemical reactions. Simultaneously, we use a parametrization of the turbulent mixing process that introduces atmospheric air to the plume. The dilution and plume cooling caused by turbulent mixing can induce drastic changes (for instance a sudden drop) of reaction rates, ultimately leading to non-equilibrium levels of several gas species. The chemical state of the plume can be tracked during the entire period of dilution and cooling to ambient atmospheric temperature.

The intensity of turbulent mixing is approximated based on viscous energy dissipation in the boundary layer (Dinger et al., 2018) and Richardson-Obukhov constant quantification by Franzese and Cassiani (2007). We examine three mixing scenarios (MSs, Figure A1), each corresponding to circular sources (e.g., bubbles bursting at the lava surface) with radii from 0.075 m (MS III) through 0.75 m (MSII) to 7.5 m (MS I) covering a substantial range of realistic emission scenarios (see Figure A1). Moreover, a coarse assessment of heterogeneity throughout the plume is possible. While MS I (slower mixing) represents the core part of larger plumes, MS III (fast mixing) accounts for the situation at the very edge of that same plume. Appendix A describes the model in detail.

The degassing scheme of open lava lakes represents an extreme (end-member-like) case of open vent volcanism, which accounts for a major fraction of volcanic gas emissions to Earth's atmosphere (Carn et al., 2017). In this study we initialize the model based on measurements at Nyiragongo lava lake (Democratic Republic of Congo). The lava lake of Nyiragongo recently was at altitudes above 3200 m (Burgi et al., 2020), corresponding to a pressure of 670 hPa, which we assume throughout this study. According to measurements of Sawyer, Carn, et al. (2008), the emitted gas is composed of H_2O (70%), CO_2 (24%), SO_2 (4.5%), CO (0.8%), OCS (0.002%), and about 0.7% of halogen species (which are ignored in the chemical mechanism used in this study). The lava temperature at Nyiragongo is ca. 1370 K (Tazieff, 1984). Based on these measurements, we calculate the TE composition (for the respectively assumed emission temperature, Figures S2 and S3 in Supporting Information S1), which is then used to initialize the kinetic model calculations. Table 1 summarizes the key chemical processes according to reaction rate analysis for different gas temperatures (see Figures S5–S20 in Supporting Information S1 for more details).

Figure 2a shows the modeled temporal evolution of the molar mixing ratios of key radicals and other plume constituents (SO_2 indicates dilution, see Figures S4a and S4b in Supporting Information S1 for more gases). For an initial temperature of 1370 K, OH amounts are already in the ppm range at the time of emission. Upon mixing with air, the OH levels further increase (to about 100 ppm) before decaying rapidly. In accordance with the processes sketched above (Figure 1) the OH peak coincides with the maximum CO conversion rate. In this example, the time scale of the respective MS determines the oxidized CO amount before it is dominated by mixing with the atmospheric background in the cooled plume.

Table 1
Selection of Key Net Chemical Conversions Within the First Moments of a Volcanic Plume as Identified by Reaction Rate Analysis of the Kinetic Model Calculations (See Figures S5–S20 in Supporting Information S1)

Reference	Reaction	Comment
I. O production from in-mixed O_2 at high T		
Ia	$SO + O_2 \rightarrow SO_2 + O$	SO, H from magm. TE
Ib	$H + O_2 \rightarrow OH + O$	–
II. OH production from O produced by Ia and Ib		
IIa	$H_2O + O \rightarrow 2\ OH$	–
III. OH conversion of plume constituents		
IIIa	$OH + CO \rightarrow CO_2 + H$	–
IIIb	$OH + H_2 \rightarrow H_2O + H$	–
IIIc	$OH + SO_2 + O_2 \rightarrow SO_3 + HO_2$	$OH + SO_2 + M \rightarrow HOSO_2 + M$
	–	$HOSO_2 + O_2 \rightarrow SO_3 + HO_2$
IV. HO_2 production from in-mixed O_2 at lower T		
IVa	$H + O_2 + M \rightarrow HO_2 + M$	–
IVb	$HOSO + O_2 \rightarrow HO_2 + SO_2$	(e.g., $SO_2 + H + M \rightarrow HOSO + M$)
V. HO_2 conversion		
Va	$HO_2 + SO_2 \rightarrow SO_3 + OH$	–
Vb	$HO_2 + HO_2 \rightarrow H_2O_2 + O_2$	($H_2O_2 + M \rightarrow 2\ OH + M$)
VI. H_2S and OCS oxidation		
VIa	$H_2S + CO_2 \rightarrow COS + H_2O$	–
VIb	$COS + O_2 \rightarrow CO + SO_2$	–

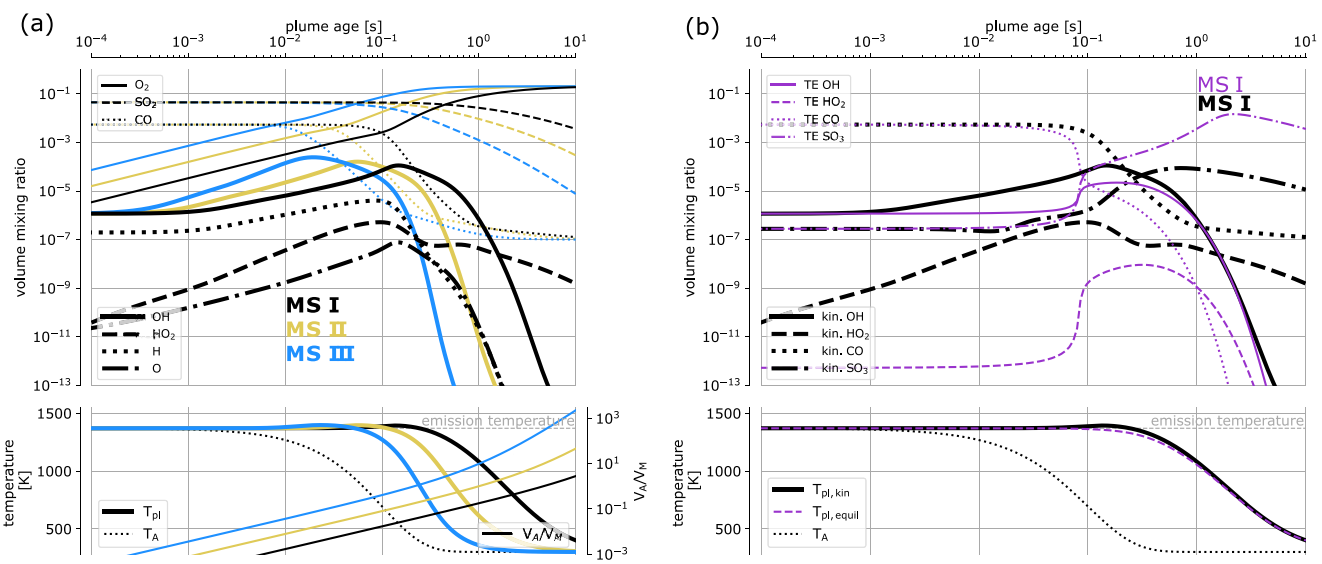

Figure 2. (a) Temporal evolution of the mixing ratios of key radicals and other plume constituents, plume temperature T_{pl}, atmospheric temperature T_A, and mixing state (given by the ratio of atmospheric air volume V_A to magmatic gas volume V_M, bottom panel) as given by the kinetic model (see Appendix A) for the three MSs (colors indicate MS I–MS III) and an emission temperature of 1370 K. In (b) the result of the kinetic simulation (MS I, thick lines) for OH, HO_2, CO, and SO_3 are shown together with the results of respective TE calculations (thin violet lines), where the composition determined by mixing was brought to TE at each time instance. High OH amounts drive gradual CO oxidation. HO_2, CO, and SO_3 show extreme deviation from the TE state. See Figure S4 in Supporting Information S1 for a plot with lower initial temperature and for further gases and MSs.

In Figure 2b the temporal evolution of the mixing ratios of OH, HO_2, CO, and SO_3 from the kinetic model run is compared to their corresponding TE mixing ratios (MS II and III in Figure S4c in Supporting Information S1). TE concentrations quickly change due to the rising O_2 amounts and the dropping temperature in the plume. The OH equilibrium levels are generally lower but follow the kinetic model rather closely, indicating that the involved reactions are fast with respect to the mixing time scales. In contrast, while TE mixing ratios of CO and HO_2 are much lower than the kinetic values, those of SO_3 are strongly enhanced. The time scales of formation or destruction of those species exceed the mixing time scale and lead to a composition of the cooled plume that depends on its early mixing history.

The rapid and mostly exothermic oxidation processes also cause considerable transient net heating of the plume (by several 10 s of K, Figure 2b), which further influences the chemistry and in part explains the remaining deviation of kinetic OH levels from TE. Plume heating through exothermic reactions was considered earlier (e.g., by Jaggar (1917), Le Guern et al. (1979)) but is rarely discussed within the scope of recent volcanic gas studies.

The importance of kinetic modeling for the investigation of high temperature magmatic gas emissions in atmospheric air has been recognized before, for example, by Martin et al. (2012), Roberts et al. (2019). Their modeling approaches already suggest the high relevance of reaction kinetics, for instance for the oxidation of reduced plume constituents. However, Martin et al. (2012) perform their calculations for constant temperatures and static volume ratios of magmatic and atmospheric gas, which is far from any realistic emission scenario. Roberts et al. (2019) coupled chemical kinetics to mixing dynamics by using a predefined scheme of plume compartments to implement a static temperature and mixing trajectory, relying on mixing parameters from external transport model calculations. They model the first 2.4 s of an explosive emission scenario, assuming a rather low emission temperature (1000 K) that varies only by about 100 K during the course of the modeled period.

Our study substantially extends the former approaches to modeling the reaction kinetics in hot volcanic gases. Full and flexible coupling of chemical kinetics to atmospheric mixing dynamics allows to cover the entire evolution of broad ranges of different realistic dynamic emission settings with only a few model runs. Thus, we can easily investigate the sensitivity of the system to different parameters (e.g., emission temperature or MS) and for instance identify different chemical regimes of a process (see Section 4). Moreover, in contrast to former approaches, we are able to assign key chemical mechanisms (i.e., the driving chemical reactions) to the results of the model calculations, which substantially improves the quality of their discussion. Further improvements over previous kinetic model studies include (a) modeling temperature influences through enthalpy changes, (b) easy adaptability and extensibility (e.g., to specific emission environments), and (c) high accessibility to the scientific community by exclusively using open-source software packages.

4. Gas Composition Changes and Emission Temperature

The temperature of the magmatic gas at the time of its emission to the atmosphere is among the major unknowns of the emission process. It depends on the lava temperature, which varies with magma type and activity and remains challenging to measure (Li et al., 2021). Moreover, it is influenced by cooling through adiabatic expansion of bubbles within the magma (Daly, 1911; Oppenheimer et al., 2018). The temperature evolution in the atmosphere is determined by fast mixing, thermal radiation, interaction with volcanic ash and aerosol, and the heat released by enthalpy changes through chemical conversions.

As shown above (Figure 2b), the OH levels of the kinetic model for high-temperature gases represent TE within about one order of magnitude. They also are in accordance with TE calculations of mixtures of magmatic and atmospheric gas assumed in earlier studies (example for 0.5 s plume age, MS I in Figure 3). The considerable range of typically observed magmatic gas compositions covered by these studies only weakly influences the OH levels, that is, they are mainly determined by temperature. For lower temperature HO_X levels are dominated by HO_2 (see also Figure S4d in Supporting Information S1) and start to become more sensitive to the abundance of reduced plume species (see blue lines in Figure 3). Hence, the emission temperature decisively determines the chemical regime of the gas emission process.

The case of CO (Figure 4a) demonstrates that the plume composition is substantially altered already a tenth of a second after emission. While reduced at high emission temperature through oxidation by OH, the CO

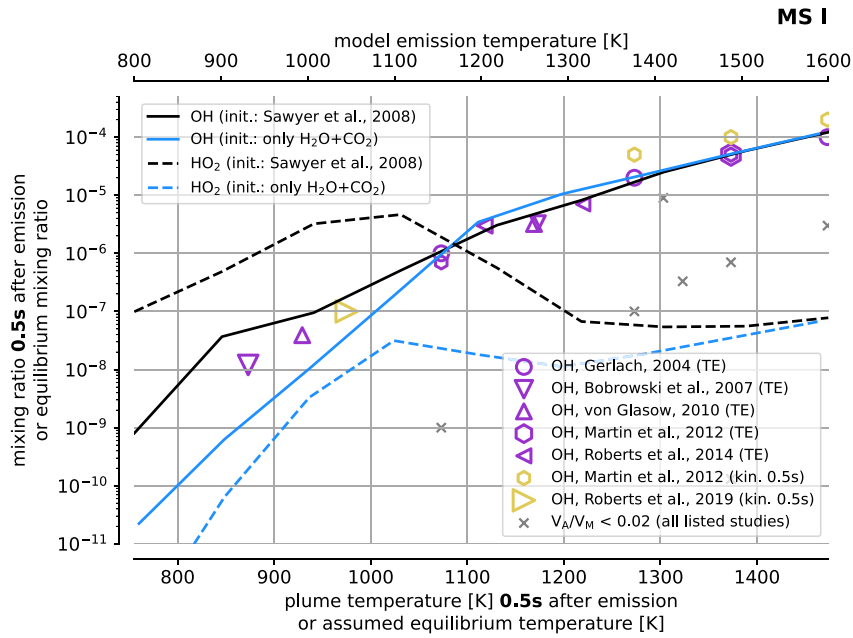

Figure 3. The modeled OH and HO_2 mixing ratio in the plume, 0.5 s after emission, plotted against its instantaneous temperature for model runs with different initial temperature for MS I. Alongside, modeled OH amounts reported in the literature are plotted. For temperatures above ca. 1000 K, OH levels are consistent with other studies that assume at least about 2% atmospheric air content (i.e., $V_A/V_M > 0.02$, all other literature values are indicated by gray crosses), without a considerable impact of the assumed initial magmatic gas composition. HO_2 levels dominate at lower temperatures. The blue lines show the results of kinetic model runs initialized with a TE of only H_2O and CO_2 (in the ratio measured by Sawyer, Carn, et al. (2008)). In this case, lower levels of reduced gases reduce HO_X levels at lower temperatures.

to CO_2 ratio increases at lower emission temperatures with respect to the initial TE value. This is due to the dominance of the fast conversion of OCS to CO (Zeng et al., 2021) and demonstrates the drastic relevance of intermediate species, which are entirely ignored in TE calculations. Consequently, redox parameters derived from measurements of magmatic gases in atmospheric air using TE relationships (e.g., the oxygen fugacity f_{O_2}, Figure 4b, Moussallam et al., 2019; Oppenheimer et al., 2018) can be either biased high (CO oxidation, emission $T >$ ca. 1100 K, up to 10 log units in the diluted plume) or low (CO formation from OCS, emission $T <$ ca. 1100 K).

Roberts et al. (2019) already showed that CO oxidation in volcanic plumes is governed by chemical kinetics, rather than TE. Our investigation of CO levels extends this finding to a broad range of emission scenarios and identifies the underlying key mechanisms. Temperature-dependent chemical regimes of the process (including an inversion in the CO level changes) could be defined and suggest that regarding the temporal evolution of individual species in a single emission scenario is not necessarily sufficient to comprehensively explain the reaction kinetics in rapidly cooling volcanic gas emissions.

Figures 4c and 4d show the ratios of different emitted gases (H_2S, OCS, and H_2) or secondary plume constituents (HO_2, H_2O_2, SO_3) to SO_2 after the plume cooled to 400 K starting from different emission temperatures. The large deviations of the gas ratios to their initial TE state at emission are induced by kinetic processes and their variation along the cooling trajectory (processes listed in Table 1 are indicated in Figure 4). The SO_3/SO_2 ratios agree with commonly measured sulfate/SO_2 ratios (see summary of literature measurements in Roberts et al. (2019)). This supports the results of Roberts et al. (2019), and extends their validity to a larger range of emission scenarios. OCS, H_2S, and H_2 levels are depleted for higher emission temperature (on split-second time scales for the assumptions made in our case study, see Figure S4 in Supporting Information S1). In contrast, HO_2 and H_2O_2 can survive plume cooling in amounts (up to 10 and 100 ppb, respectively) exceeding initial TE levels (sub-ppt levels for $T <$ 1300 K, see Figure S2 in Supporting Information S1) and atmospheric background levels (ca. 10 ppt for HO_2 and 2–6 ppb for H_2O_2, see Seinfeld and Pandis (2006)).

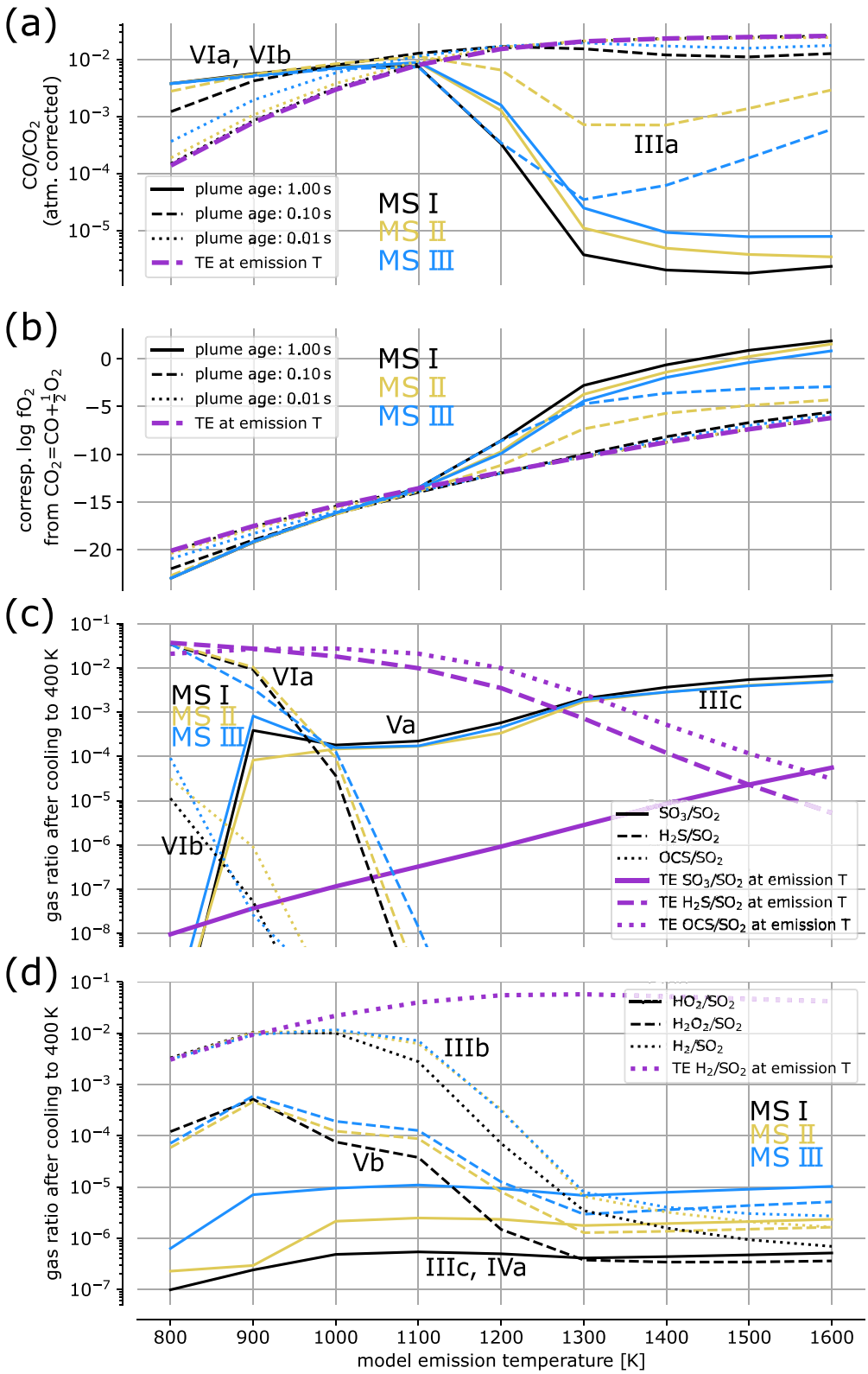
(a)
CO/CO2 (atm. corrected)
VIa, VIb
IIIa
plume age: 1.00 s
plume age: 0.10 s
plume age: 0.01 s
TE at emission T
MS I
MS II
MS III
(b)
corresp. log fO2 from CO2=CO+½O2
(c)
gas ratio after cooling to 400 K
VIa
Va
IIIc
VIb
SO3/SO2
H2S/SO2
OCS/SO2
TE SO3/SO2 at emission T
TE H2S/SO2 at emission T
TE OCS/SO2 at emission T
(d)
HO2/SO2
H2O2/SO2
H2/SO2
TE H2/SO2 at emission T
IIIb
Vb
IIIc, IVa
model emission temperature [K]

Figure 4.

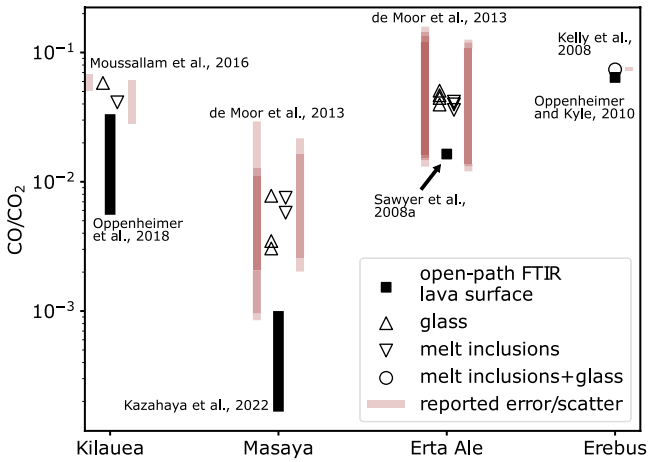

Figure 5. CO to CO_2 ratios measured at four lava lakes (at Kilauea, Masaya, Erta Ale, and Erebus volcano) by open-path Fourier transform infrared spectroscopy (FTIR) using lava thermal emission as light source (data from Oppenheimer et al. (2018), Kazahaya et al. (2022), Sawyer, Oppenheimer, et al. (2008), Oppenheimer and Kyle (2008)). The values are systematically lower than those expected from the melt equilibrium, which are calculated based on melt temperature and the oxygen fugacity of melt inclusions and matrix glasses (data from Moussallam et al. (2016), de Moor et al. (2013), Kelly et al. (2008), calculations base on the thermodynamic equilibrium of $CO + \frac{1}{2}O_2 = CO_2$ with thermochemical data by Allison (2013)). See Table S2 in Supporting Information S1 for more details.

5. Implications for Volcanic Gas Studies

Our modeling of the reaction kinetics of high-temperature volcanic gas emissions reveals fundamental inconsistencies between state-of-the-art chemical knowledge (i.e., reaction rate constants and reaction kinetics) and common interpretations of volcanic degassing processes. Examples include:

1. H_2S, H_2, and CO have been observed in seconds-to-minutes-old volcanic plumes (e.g., Aiuppa et al., 2007, 2011; Schumann et al., 2011). However, their abundance is in most cases not compatible with TE considerations. So far, these inconsistencies are explained by stating that some of the emitted species "re-equilibrate" (with the atmosphere) and others do not (e.g., Aiuppa et al., 2011; Martin et al., 2009). Furthermore, these studies suggest that the hot and direct emission of magmatic gases to the atmosphere might lead to quenching of the TE levels of reduced magmatic gases in the plume. Our results show that many of the magmatic species are likely to be present in amounts that substantially deviate from both, magmatic TE and TE of the plume (i.e., the mixture of magmatic gases and atmospheric air). Moreover, our results show that the direct intrusion of O_2 into hot magmatic gas emissions significantly enhances the oxidation of reduced magmatic species (Figure 4). The introduction of kinetic processes and intermediate species to the discussion will considerably refine the interpretations of former and future volcanic gas measurements at open vents. Volcano-specific adaptions of our model (e.g., lowered O_2 levels in vent systems) will support the interpretation of measurements of reduced plume species (and also that of sulfate, Roberts et al. (2019)).
2. High-temperature volcanic gas measurements are thought to be representative for the magmatic gas redox state, which, in turn, is assumed to equal the redox state of their formerly hosting magmas (Giggenbach, 1996). The compositions of "disequilibrium" samples of hot plume gases (i.e., samples that did not resemble a TE state) are modified in retrospect to conform to a TE state in so-called "restoration" procedures (see e.g., Gerlach, 1980, 1993; Symonds et al., 1994). By assuming that levels of reduced species are lowered through atmospheric oxidation and oxygen mass balance calculations, high-temperature fumarole gas emission samples could be corrected consistently for the influence of atmospheric contamination (e.g., de Moor et al., 2013). Our model results confirm that these assumptions are very likely to be valid at high emission temperatures (see Figure 4). However, particularly for lower emission temperatures the influence of remaining intermediate species (for instance CO produced by OCS oxidation, see Figure 4a) and other details of chemical kinetics can cause substantial uncertainties in such approaches. This could introduce biases in these data, which are widely used, for instance in studies on the evolution of the early Earth's atmosphere (Holland, 2002).
3. We find a strong influence of reaction kinetics on the magmatic redox state as derived from volcanic plume gas samples (e.g., f_{O_2} determined from redox pairs in a 0.1 s old plume, Figure 4b). The magmatic gas composition after emission is governed by emission temperature and degassing style (MSs are related to bubble sizes). For higher emission temperatures ($T >$ ca. 1100 K) CO oxidation leads to reduced CO to CO_2 ratios. Figure 5 shows CO to CO_2 ratios as measured at four different lava lakes by open-path Fourier transform infrared spectroscopy (FTIR). A systematic bias to low CO to CO_2 ratios is observed, when comparing the values to the ratios calculated using melt temperature and the oxygen fugacities derived from respective melt inclusions and matrix glasses. The discrepancy between observed gas redox states and those of the hosting melts was previously solely attributed to thermal decoupling of gas bubbles from the surrounding magma (Moussallam et al., 2019; Oppenheimer et al., 2018). Open-path infrared measurements using the thermal emission of the lava surface as light source sample the magmatic gas slightly after its first contact to atmospheric air. An influence of the fast oxidation processes studied here is likely to be unavoidable for this

Figure 4. Panel (a) shows volcanic molar CO/CO_2 as a function of gas emission temperature for different MSs and at different plume age. The influence of mixing with atmospheric CO and CO_2 is corrected. (b) Logarithmic oxygen fugacity f_{O_2} calculated from the CO/CO_2 values in (a) (equilibrium constant calculated using thermochemical data from Allison (2013)). (c) Modeled SO_3, H_2S, and OCS amount normalized to SO_2 after cooling of the plume to 400 K, starting from different model emission temperatures and assuming different MSs. (d) Same as (c) for HO_2, H_2O_2, and H_2. Within the plots references to the relevant kinetic processes (roman numbers, Table 1) are provided.

measurement approach. Future studies should focus on the quantification of the relative relevance of decoupling between gas and melt redox state and fast chemical conversion in the magma-atmosphere interface for open vent emissions.

4. Models of reactive halogen chemistry in the minutes-to-hours-old plume strongly depend on the radical amount, particularly HO_2, in the initial plume composition (Surl et al., 2021). Previous reactive halogen studies always used high-temperature TE calculations to initiate the plume model (Bobrowski et al., 2007; Roberts et al., 2014; Surl et al., 2021; von Glasow, 2010), typically resulting in HO_X levels in the ppm range. With the considerably lower HO_2 levels (ppb range) and the depleted OH levels in the cooled plume, indicated by our kinetic simulations, reactive halogen plume models might no longer reproduce the observed bromine monoxide levels. Including halogens into the chemical mechanism of our model will enable a straight-forward and entirely kinetic treatment of halogen chemistry in volcanic plumes. Providing such fundamental constraints to the models will lead to a substantial refinement of the understanding of phenomena that arise from the interaction of atmospheric air and magmatic gases in downwind plumes.

Open vent volcanic gas emissions are challenging to study and there remain major uncertainties in the determining parameters of the process (e.g., emission temperature, atmospheric turbulence, reaction rate constants). By introducing a comprehensive and flexible framework for simulating dynamic gas emission processes with steep temperature gradients, we are able to unveil central kinetic processes at the interface between magma and the atmosphere. We show that these processes can determine the gas composition of volcanic plumes by altering the magmatic gas composition within split-seconds after their emission. Since the time scales of mixing and high-temperature chemical conversion are comparable, the abundance of many plume constituents deviate by orders of magnitude from the amount expected by both, the initial magmatic TE and the TE of the plume. Moreover, kinetic processes influence the plume temperature by the enthalpy changes introduced by the chemical reactions. Evaluations and interpretations of volcanic gas measurements at open vents will strongly benefit from considering high-temperature reaction kinetics and emission dynamics in volcano-specific adaptions of the here described model. Further progress is expected from considering more details of spatial heterogeneity, including heterogeneous chemistry, and adding further gas species to the model and, most notably, from improved and dedicated field observations to validate and better constrain the model calculations (e.g., OH measurements, see Kuhn et al., 2021).

Appendix A: A Model for the Assessment of Early-Stage Volcanic Gas Emissions

We introduce a model that covers large ranges of turbulent mixing scenarios by a simple but comprehensive parametrization and combines it with a kinetic treatment of the relevant chemical mechanisms. The model allows to identify the driving chemical processes inside the plume during the entire cooling period and to study their sensitivity on parameters such as the gas emission temperature for different turbulent mixing scenarios.

We use a 1-box approach to calculate the plume's chemical composition $\vec{c}_{pl}$ (concentrations in mol cm^{-3}) and temperature T_{pl} (in K) as a function of time t. A stationary emission plume with circular cross section is assumed with advection determining the transport along the plume axis and neglecting mixing in that direction. The process is then basically governed by lateral mixing with the atmosphere and chemistry, so that for a given set of initial values $\left(\vec{c}_{pl,0}, T_{pl,0}\right)$ the progression of plume composition and temperature can be inferred numerically through integration of the two derivatives:

$$\frac{dT_{pl}}{dt} = \left.\frac{dT_{pl}}{dt}\right|_{mix} + \left.\frac{dT_{pl}}{dt}\right|_{chem} \tag{A1}$$

$$\frac{d\vec{c}_{pl}}{dt} = \left.\frac{d\vec{c}_{pl}}{dt}\right|_{mix} + \left.\frac{d\vec{c}_{pl}}{dt}\right|_{chem} \tag{A2}$$

A1. Mixing

The plume box expands with time and at any time includes all the emitted gas molecules (see also von Glasow et al., 2003). Turbulence will cause an absolute dispersion of the plume, consisting of both meandering and relative dispersion with respect to its center of mass. The relative plume dispersion is driven by in-mixing of the

surrounding air. For young plumes (plume diameter not exceeding several tens of meters), the increase of plume size leads to an increase of (larger) turbulence elements (eddies) contributing to mixing instead of meandering, thereby causing an accelerated plume growth with time (Batchelor, 1952). With the assumption of isotropic turbulence and characteristic plume sizes within the so-called "inertial subrange" (i.e., some mm up to hundreds of m in the atmosphere (MacCready, 1962)), the mean squared displacement of a plume element from its center of mass $\sigma^2_{\mathrm{pl,rel}}$ can be approximated by Franzese and Cassiani (2007):

$$\sigma^2_{\mathrm{pl,rel}} = C\epsilon(t + t_\mathrm{s})^3 \tag{A3}$$

C is the Richardson-Obukhov constant accounting for the turbulence scenario and ϵ denotes the viscous energy dissipation. Franzese and Cassiani (2007) argue that the emission of sources of finite sizes (radius r_0) can be approximated using a translation t_s of the time origin of the point source emission case (i.e., $t_\mathrm{s} = 0$). The emission plume of a source with given radius r_0 is then described by the plume of a point source after the time t_s that it takes the average displacement of plume particles to reach the source size r_0. t_s is given by

$$t_\mathrm{s} = \left(r_0^2/C\epsilon\right)^{1/3} \tag{A4}$$

(which is obtained by setting $\sigma_{\mathrm{pl,rel}} = r_0$ in Equation A3).

The situation, for instance at a gas emitting lava lake is certainly more complex. Turbulence might not be isotropic and the turbulence scenario, as well as the viscous energy dissipation are difficult to quantify. Nevertheless and because slightly accelerated plume growth fits observations in nature, we will use Equation A3 to quantify the expansion of the plume box in our model. We combine $C\epsilon$ to a parameter γ, which has the dimension of an energy dissipation ($\mathrm{m^2\ s^{-3}}$) and parameterizes the strength of turbulent mixing. Together with the effective initial source radius r_0 the plume geometry (plume radius r) is described by:

$$r(t) = \sqrt{\gamma(t_\mathrm{s} + t)^3} \tag{A5}$$

From geometrical considerations and assuming the atmosphere to be a static reservoir for atmospheric gases, temperature, and pressure, the mixing terms in Equations A1 and A2 can be derived as (see Supplementary Note 1 in Supporting Information S1):

$$\left.\frac{\mathrm{d}T_\mathrm{pl}}{\mathrm{d}t}\right|_\mathrm{mix} = 3(t_\mathrm{s} + t)^{-1}\beta\left(T_\mathrm{A} - T_\mathrm{pl}\right) \tag{A6}$$

$$\left.\frac{\mathrm{d}\vec{c}_\mathrm{pl}}{\mathrm{d}t}\right|_\mathrm{mix} = 3(t_\mathrm{s} + t)^{-1}\left(\vec{c}_\mathrm{A} - \vec{c}_\mathrm{pl}\right) \tag{A7}$$

T_A and $\vec{c}_\mathrm{A}$ represent the temperature and composition of the atmospheric reservoir. The factor β contains the ratio of specific heat per unit volume of the atmosphere to that of the plume. The mixing process is described by a single parameter that is the temporal translation of the point source emission case t_s, which depends on the ratio of r_0 and γ (see Equation A4). Thereby, within a specific model mixing scenario (MS, determined by the choice of t_s) uncertainties in the turbulent mixing process are absorbed by a slight variation of the bubble radius. Or, one MS describes the situation for the range of bubble radii linked (via t_s) to realistic turbulence scenarios (see Table S1 in Supporting Information S1 for examples).

In this mixing scheme, there remains a slight imbalance between the expansion of the in-mixed and quickly heated atmospheric air and the contraction of the slightly cooled plume gas. This effect (details in Supplementary Note 2 in Supporting Information S1) will lead to a slight plume expansion (<25% in the more extreme cases used in this study) and thus, to a deviation of the real plume volume to that determined by Equation A5. The associated inaccuracy is minor regarding the high level of simplification of the model and has a negligible effect on the results as these only rely on intensive quantities.

The state of mixing is commonly given by the ratio M of the volume of atmospheric gas that is mixed into the plume V_A to that of the initial gas emission (magmatic gas) V_M (Gerlach, 2004). For the assumptions made here it can be calculated as:

$$M(t) = \frac{V_A(t)}{V_M} = \frac{r(t)^2}{r_0^2} - 1 \tag{A8}$$

The hot lava impacts atmospheric temperature right above its surface and close to the location of gas emission. This is accounted for by a fast exponential decay (time constant $\tau = 0.1$ s) of T_A from magmatic gas temperature to the atmospheric temperature $T_{A,\infty}$ far from the lava surface (see Figures A1c and 1):

$$T_A = T_{A,\infty} + \left(T_{pl} - T_{A,\infty}\right) \exp\left(-\frac{t}{\tau}\right) \tag{A9}$$

This process is implemented as a static boundary condition to the model. Figure A1 illustrates the mixing process of the MS used in this study.

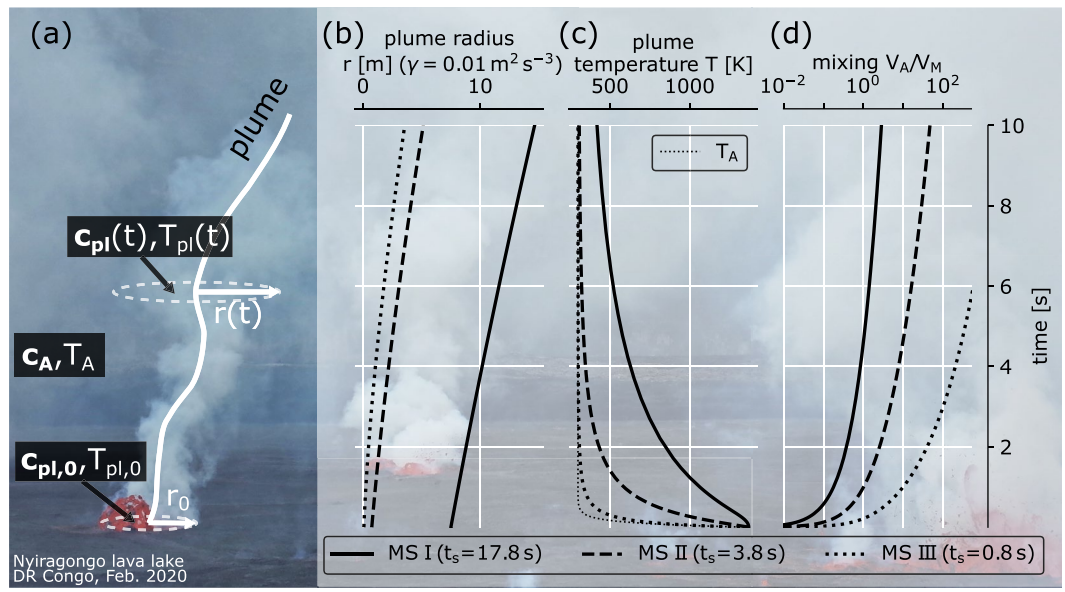

Figure A1. A parametrized increase of the radius of the assumed circular plume box drives mixing in the model. This is schematically illustrated in panel (a). Plume radius (b), temperature (c) and mixing (d) are shown for the three MSs assumed in this study. The diameter of the bubble in the background photo of panel (a) occupies 230 pixels. The image was taken with a focal length of 18.3 mm, a detector with 25.1 mm and 3,936 pixels horizontal dimension at a distance of about 20–50 m. Thus, the radius of the bubble is ca. 0.8–2 m, close to MS II for $\gamma = 0.01 m^2\,s^{-3}$.

A2. Chemistry

Chemical conversion rates as well as thermodynamic data of the gas species can be found in numerous literature reaction mechanism compilations. Reaction mechanisms in volcanic gas emissions are - to some extent—similar to processes in combustion chemistry, which are well studied due to their importance in many branches of engineering. In this study, we use the C-H-O-S combustion mechanism of Zeng et al. (2021), which is based on former work of for example, (Glarborg et al., 2014). The mechanism includes the major volcanic plume constituents, except for halogen or reactive nitrogen species. We removed a H_2O-SO_2 van der Waals complex from the mechanism of Zeng et al. (2021) since, due to the respective fast reaction rates and the large amounts and variations of H_2O and SO_2, it disturbed the analysis of the conversion rates during the cooling process. The complex solely modified H_2O and SO_2 levels by a factor of about 10^{-4} and is thus negligible for this study.

The reaction mechanism is compiled with the open-source software package Cantera (Goodwin et al., 2021). The chemical conversion rates (second term on the right hand side in Equation A2) are calculated from all the reactions in the mechanism for the instantaneous plume state. At the same time the temperature influence through chemistry (second term on the right hand side in Equation A1) is calculated according to

$$\left.\frac{dT_{pl}}{dt}\right|_{chem} = \frac{1}{s_{p,pl}\,\rho_{pl}} \sum_i h_i \left.\frac{dc_{pl,i}}{dt}\right|_{chem} \quad \text{(A10)}$$

from the molar enthalpies h (in J molec^{-1}) and the conversion rates of all species i, the density ρ_{pl} (in molec cm^{-3}), and specific heat capacity $s_{p,pl}$ (in J K^{-1} molec^{-1}) of the plume.

For given initial conditions and mixing parameters the model is solved by an ordinary differential equation solver. We used a backward differentiation formula method (Curtiss & Hirschfelder, 1952) implemented in the SciPy package (Virtanen et al., 2020) in Python. Depending on the chemical mechanism used, a single run modeling the first plume seconds (covering the entire cooling period) takes on the order of a second on a personal computer from the year 2012 (1.9 GHz).

Besides kinetic studies, the Cantera software also enables the calculation of TE in gas mixtures for example, for a given temperature and pressure. This is used to compare TE with kinetic results.

A3. Limitations of Volcanic Gas Emission Models

The simplifications made by the model enable a comprehensive study and reasonable quantitative approximation of the volcanic gas emission process. On the other hand, they call for due care, when interpreting the results. However, the analysis of uncertainties has to encompass both, the simplifications made by the model and the major uncertainties and unknowns concerning the initial conditions. The latter are significant due to the coarsely studied and hardly approachable processes of the degassing interface of hot magma and the atmosphere.

The major simplifications made by the model are:

1. The 1-box implementation of the model assumes spatial homogeneity across the plume cross section for each MS. In reality large (concentration and temperature) gradients across the plume might severely influence the chemistry in the early plume. Evaluating different MSs enables an approximate treatment of spatial in-homogeneity.
2. The plume temperature is likely to be influenced by processes other than mixing and chemistry (as assumed in the model, see Equation A1), for instance thermal radiation effects or interactions with ash and aerosol particles.
3. The chemistry mechanism used in this model study only includes gas-phase C-H-O-S species. Halogens and reactive nitrogen chemistry, as well as heterogeneous chemistry is not considered.

The basic uncertainties concerning the involved processes - and thereby the initial conditions or boundary conditions - include:

1. The degassing temperature of the gas is very challenging to quantify, as it might be influenced by for example, thermal radiation and adiabatic expansion. Direct measurements of absolute lava temperature are scarce and recently Li et al. (2021) found that they are bound to large uncertainties (exceeding 100 K) when relying on the thermal emissivity.
2. The initial composition of magmatic gases used in the model could be a further factor of uncertainty. Only a few plume species can be quantified reliably with today's sampling techniques. Furthermore, depending on the sampling technique, the measured gas composition could have been substantially altered between emission and the time of sampling (through the processes discussed in this study). Regarding the fact that bubble evolution can also be highly dynamic (Oppenheimer et al., 2018), it can even be questioned whether, prior to emission, the magmatic gas composition is in TE at all.
3. The rate constants of many reactions used in the chemical mechanism are subject to considerable uncertainties, particularly for high temperature (Glarborg et al., 2014; Roberts et al., 2019; Zeng et al., 2021). And, the impact of possible heterogeneous reactions on the surface of volcanic ash and aerosol particles on high-temperature chemistry is largely unknown.

The listed uncertainties in the degassing processes justify the simplifications made in our model to a large extent. Improving the model, for example, with respect to its spatial resolution or its temperature dependencies, would not significantly reduce the overall uncertainties of the results, since they are substantially determined by unknown boundary and initial conditions. Nevertheless, our model includes the major plume species and a flex-

ible parametrization of turbulent mixing allows the coverage of huge ranges of initial and boundary conditions within only a few model runs. The results of our kinetic calculations deviate from those of TE calculations by many orders of magnitude. The model uncertainties are thus unlikely to influence the basic findings and conclusions of this study.

Data Availability Statement

The kinetic data used in this study is available as supplementary data of the open access article by Zeng et al. (2021). We used the open source Cantera software package (Goodwin et al., 2021) to implement the model as described in detail in Appendix A.

Acknowledgments
We thank Evgenia Ilyinskaya, Tobias Fischer, and Christoph Kern for their valuable comments and suggestions during the review process. This research has been partially funded by the German Research Foundation (DFG; project no. PL 193/23-1). Open Access funding enabled and organized by Projekt DEAL.

References

Aiuppa, A., Franco, A., von Glasow, R., Allen, A. G., D'Alessandro, W., Mather, T. A., et al. (2007). The tropospheric processing of acidic gases and hydrogen sulphide in volcanic gas plumes as inferred from field and model investigations. *Atmospheric Chemistry and Physics*, *7*(5), 1441–1450. https://doi.org/10.5194/acp-7-1441-2007

Aiuppa, A., Shinohara, H., Tamburello, G., Giudice, G., Liuzzo, M., & Moretti, R. (2011). Hydrogen in the gas plume of an open-vent volcano, Mount Etna, Italy. *Journal of Geophysical Research*, *116*(B10), B10204. https://doi.org/10.1029/2011jb008461

Allison, T. C. (2013). *NIST-JANAF thermochemical tables—SRD 13*. National Institute of Standards and Technology. https://doi.org/10.18434/T42S31

Batchelor, G. K. (1952). Diffusion in a field of homogeneous turbulence. *Mathematical Proceedings of the Cambridge Philosophical Society*, *48*(2), 345–362. https://doi.org/10.1017/s0305004100027687

Bobrowski, N., von Glasow, R., Aiuppa, A., Inguaggiato, S., Louban, I., Ibrahim, O. W., & Platt, U. (2007). Reactive halogen chemistry in volcanic plumes. *Journal of Geophysical Research*, *112*(D6), D06311. https://doi.org/10.1029/2006jd007206

Bonhoeffer, K. F., & Reichardt, H. (1928). Zerfall von erhitztem Wasserdampf in Wasserstoff und freies Hydroxyl. *Zeitschrift für Physikalische Chemie*, *139A*(1), 75–97. https://doi.org/10.1515/zpch-1928-13909

Burgi, P.-Y., Boudoire, G., Rufino, F., Karume, K., & Tedesco, D. (2020). Recent activity of nyiragongo (Democratic Republic of Congo): New insights from field observations and numerical modeling. *Geophysical Research Letters*, *47*(17), e2020GL088484. https://doi.org/10.1029/2020gl088484

Carn, S. A., Fioletov, V. E., McLinden, C. A., Li, C., & Krotkov, N. A. (2017). A decade of global volcanic SO_2 emissions measured from space. *Scientific Reports*, *7*, 1. https://doi.org/10.1038/srep44095

Cattolica, R. J., Yoon, S., & Knuth, E. L. (1982). OH concentration in an atmospheric-pressure methane-air flame from molecular-beam mass spectrometry and laser-absorption spectroscopy. *Combustion Science and Technology*, *28*(5–6), 225–239. https://doi.org/10.1080/00102208208952557

Crutzen, P. J. (1974). Photochemical reactions initiated by and influencing ozone in unpolluted tropospheric air. *Tellus*, *26*(1–2), 47–57. https://doi.org/10.3402/tellusa.v26i1-2.9736

Curtiss, C. F., & Hirschfelder, J. O. (1952). Integration of stiff equations. *Proceedings of the National Academy of Sciences of the United States of America*, *38*(3), 235–243. https://doi.org/10.1073/pnas.38.3.235

Daly, R. A. (1911). The nature of volcanic action. *Proceedings of the American Academy of Arts and Sciences*, *47*(3), 47. https://doi.org/10.2307/20022712

de Moor, J. M., Fischer, T. P., Sharp, Z. D., King, P. L., Wilke, M., Botcharnikov, R. E., et al. (2013). Sulfur degassing at Erta Ale (Ethiopia) and Masaya (Nicaragua) volcanoes: Implications for degassing processes and oxygen fugacities of basaltic systems. *Geochemistry, Geophysics, Geosystems*, *14*(10), 4076–4108. https://doi.org/10.1002/ggge.20255

Dinger, A. S., Stebel, K., Cassiani, M., Ardeshiri, H., Bernardo, C., Kylling, A., et al. (2018). Observation of turbulent dispersion of artificially released SO_2 puffs with UV cameras. *Atmospheric Measurement Techniques*, *11*(11), 6169–6188. https://doi.org/10.5194/amt-11-6169-2018

Franzese, P., & Cassiani, M. (2007). A statistical theory of turbulent relative dispersion. *Journal of Fluid Mechanics*, *571*, 391–417. https://doi.org/10.1017/s0022112006003375

Gaillard, F., Scaillet, B., & Arndt, N. T. (2011). Atmospheric oxygenation caused by a change in volcanic degassing pressure. *Nature*, *478*(7368), 229–232. https://doi.org/10.1038/nature10460

Gerlach, T. M. (1980). Chemical characteristics of the volcanic gases from Nyiragongo lava lake and the generation of CH4-rich fluid inclusions in alkaline rocks. *Journal of Volcanology and Geothermal Research*, *8*(2–4), 177–189. https://doi.org/10.1016/0377-0273(80)90103-1

Gerlach, T. M. (1993). Thermodynamic evaluation and restoration of volcanic gas analyses: An example based on modern collection and analytical methods. *Geochemical Journal*, *27*(4/5), 305–322. https://doi.org/10.2343/geochemj.27.305

Gerlach, T. M. (2004). Volcanic sources of tropospheric ozone-depleting trace gases. *Geochemistry, Geophysics, Geosystems*, *5*, Q09007. https://doi.org/10.1029/2004gc000747

Gerlach, T. M., & Nordlie, B. E. (1975). The C-O-H-S gaseous system; part II, temperature, atomic composition, and molecular equilibria in volcanic gases. *American Journal of Science*, *275*(4), 377–394. https://doi.org/10.2475/ajs.275.4.377

Giggenbach, W. F. (1987). Redox processes governing the chemistry of fumarolic gas discharges from White Island, New Zealand. *Applied Geochemistry*, *2*(2), 143–161. https://doi.org/10.1016/0883-2927(87)90030-8

Giggenbach, W. F. (1996). Chemical composition of volcanic gases. In *Monitoring and mitigation of volcano hazards* (pp. 221–256). Springer Berlin Heidelberg. https://doi.org/10.1007/978-3-642-80087-0_7

Glarborg, P., Halaburt, B., Marshall, P., Guillory, A., Troe, J., Thellefsen, M., & Christensen, K. (2014). Oxidation of reduced sulfur species: Carbon disulfide. *The Journal of Physical Chemistry A*, *118*(34), 6798–6809. https://doi.org/10.1021/jp5058012

Goodwin, D. G., Speth, R. L., Moffat, H. K., & Weber, B. W. (2021). Cantera: An object-oriented software toolkit for chemical kinetics, thermodynamics, and transport processes. https://doi.org/10.5281/zenodo.4527812

Henley, R. W., & Fischer, T. P. (2021). Sulfur sequestration and redox equilibria in volcanic gases. *Journal of Volcanology and Geothermal Research*, *414*, 107181. https://doi.org/10.1016/j.jvolgeores.2021.107181

Holland, H. D. (2002). Volcanic gases, black smokers, and the great oxidation event. *Geochimica et Cosmochimica Acta*, *66*(21), 3811–3826. https://doi.org/10.1016/s0016-7037(02)00950-x

Jaggar, T. A. (1917). Volcanologic investigations at Kilauea. *American Journal of Science*, *s4–44*(261), 161–220. https://doi.org/10.2475/ajs.s4-44.261.161

Kasting, J. F. (1993). Earth's early atmosphere. *Science*, *259*(5097), 920–926. https://doi.org/10.1126/science.11536547

Kazahaya, R., Varnam, M., Esse, B., Burton, M., Shinohara, H., & Ibarra, M. (2022). Behaviors of redox-sensitive components in the volcanic plume at Masaya volcano, Nicaragua: H_2 oxidation and CO preservation in air. *Frontiers of Earth Science*, *10*. https://doi.org/10.3389/feart.2022.867562

Kelly, P. J., Kyle, P. R., Dunbar, N. W., & Sims, K. W. W. (2008). Geochemistry and mineralogy of the phonolite lava lake, Erebus volcano, Antarctica: 1972–2004 and comparison with older lavas. *Journal of Volcanology and Geothermal Research*, *177*(3), 589–605. https://doi.org/10.1016/j.jvolgeores.2007.11.025

Kuhn, J., Bobrowski, N., Wagner, T., & Platt, U. (2021). Mobile and high-spectral-resolution Fabry–Pérot interferometer spectrographs for atmospheric remote sensing. *Atmospheric Measurement Techniques*, *14*(12), 7873–7892. https://doi.org/10.5194/amt-14-7873-2021

Le Guern, F., Carbonnelle, J., & Tazieff, H. (1979). Erta'ale lava lake: Heat and gas transfer to the atmosphere. *Journal of Volcanology and Geothermal Research*, *6*(1–2), 27–48. https://doi.org/10.1016/0377-0273(79)90045-3

Levy, H. (1971). Normal atmosphere: Large radical and formaldehyde concentrations predicted. *Science*, *173*(3992), 141–143. https://doi.org/10.1126/science.173.3992.141

Li, H., Andujar, J., Slodczyk, A., Meneses, D. D. S., Scaillet, B., Echegut, P., et al. (2021). Spectral emissivity of phonolite lava at high temperature. *IEEE Transactions on Geoscience and Remote Sensing*, *60*, 1–15. https://doi.org/10.1109/tgrs.2021.3104657

MacCready, P. B. (1962). The inertial subrange of atmospheric turbulence. *Journal of Geophysical Research*, *67*(3), 1051–1059. https://doi.org/10.1029/jz067i003p01051

Martin, R., Ilyinskaya, E., & Oppenheimer, C. (2012). The enigma of reactive nitrogen in volcanic emissions. *Geochimica et Cosmochimica Acta*, *95*, 93–105. https://doi.org/10.1016/j.gca.2012.07.027

Martin, R., Mather, T. A., & Pyle, D. M. (2006). High-temperature mixtures of magmatic and atmospheric gases. *Geochemistry, Geophysics, Geosystems*, *7*, Q04006. https://doi.org/10.1029/2005gc001186

Martin, R., Roberts, T., Mather, T., & Pyle, D. (2009). The implications of H2S and H2 kinetic stability in high-t mixtures of magmatic and atmospheric gases for the production of oxidized trace species (e.g., BrO and NOx). *Chemical Geology*, *263*(1–4), 143–150. https://doi.org/10.1016/j.chemgeo.2008.12.028

Moussallam, Y., Edmonds, M., Scaillet, B., Peters, N., Gennaro, E., Sides, I., & Oppenheimer, C. (2016). The impact of degassing on the oxidation state of basaltic magmas: A case study of Kīlauea volcano. *Earth and Planetary Science Letters*, *450*, 317–325. https://doi.org/10.1016/j.epsl.2016.06.031

Moussallam, Y., Oppenheimer, C., & Scaillet, B. (2019). On the relationship between oxidation state and temperature of volcanic gas emissions. *Earth and Planetary Science Letters*, *520*, 260–267. https://doi.org/10.1016/j.epsl.2019.05.036

Oppenheimer, C., & Kyle, P. R. (2008). Probing the magma plumbing of Erebus volcano, Antarctica, by open-path FTIR spectroscopy of gas emissions. *Journal of Volcanology and Geothermal Research*, *177*(3), 743–754. https://doi.org/10.1016/j.jvolgeores.2007.08.022

Oppenheimer, C., Scaillet, B., Woods, A., Sutton, A. J., Elias, T., & Moussallam, Y. (2018). Influence of eruptive style on volcanic gas emission chemistry and temperature. *Nature Geoscience*, *11*(9), 678–681. https://doi.org/10.1038/s41561-018-0194-5

Roberts, T., Dayma, G., & Oppenheimer, C. (2019). Reaction rates control high-temperature chemistry of volcanic gases in air. *Frontiers of Earth Science*, *7*, 159. https://doi.org/10.3389/feart.2019.00154

Roberts, T., Martin, R., & Jourdain, L. (2014). Reactive bromine chemistry in Mount Etna's volcanic plume: The influence of total Br, high-temperature processing, aerosol loading and plume–air mixing. *Atmospheric Chemistry and Physics*, *14*(20), 11201–11219. https://doi.org/10.5194/acp-14-11201-2014

Robock, A. (2000). Volcanic eruptions and climate. *Reviews of Geophysics*, *38*(2), 191–219. https://doi.org/10.1029/1998rg000054

Sawyer, G. M., Carn, S. A., Tsanev, V. I., Oppenheimer, C., & Burton, M. (2008). Investigation into magma degassing at Nyiragongo volcano, Democratic Republic of the Congo. *Geochemistry, Geophysics, Geosystems*, *9*, Q02017. https://doi.org/10.1029/2007gc001829

Sawyer, G. M., Oppenheimer, C., Tsanev, V. I., & Yirgu, G. (2008). Magmatic degassing at Erta 'ale volcano, Ethiopia. *Journal of Volcanology and Geothermal Research*, *178*(4), 837–846. https://doi.org/10.1016/j.jvolgeores.2008.09.017

Schumann, U., Weinzierl, B., Reitebuch, O., Schlager, H., Minikin, A., Forster, C., et al. (2011). Airborne observations of the Eyjafjalla volcano ash cloud over Europe during air space closure in April and May 2010. *Atmospheric Chemistry and Physics*, *11*(5), 2245–2279. https://doi.org/10.5194/acp-11-2245-2011

Seinfeld, J. H., & Pandis, S. N. (2006). *Atmospheric chemistry and physics: From air pollution to climate change* (2nd ed.). John Wiley and Sons, Inc.

Surl, L., Roberts, T., & Bekki, S. (2021). Observation and modelling of ozone-destructive halogen chemistry in a passively degassing volcanic plume. *Atmospheric Chemistry and Physics*, *21*(16), 12413–12441. https://doi.org/10.5194/acp-21-12413-2021

Symonds, R. B., Rose, W. I., Bluth, G. J. S., & Gerlach, T. M. (1994). Volcanic-gas studies; methods, results, and applications. *Reviews in Mineralogy and Geochemistry*, *30*(1), 1–66.

Tazieff, H. (1984). Mt. Niragongo: Renewed activity of the lava lake. *Journal of Volcanology and Geothermal Research*, *20*(3–4), 267–280. https://doi.org/10.1016/0377-0273(84)90043-x

Virtanen, P., Gommers, R., Oliphant, T. E., Haberland, M., Reddy, T., Cournapeau, D., et al. (2020). SciPy 1.0: Fundamental algorithms for scientific computing in python. *Nature Methods*, *17*(3), 261–272. https://doi.org/10.1038/s41592-019-0686-2

von Glasow, R. (2010). Atmospheric chemistry in volcanic plumes. *Proceedings of the National Academy of Sciences of the United States of America*, *107*(15), 6594–6599. https://doi.org/10.1073/pnas.0913164107

von Glasow, R., Lawrence, M. G., Sander, R., & Crutzen, P. J. (2003). Modeling the chemical effects of ship exhaust in the cloud-free marine boundary layer. *Atmospheric Chemistry and Physics*, *3*(1), 233–250. https://doi.org/10.5194/acp-3-233-2003

Willbourn, A. H., & Hinshelwood, C. N. (1946). The mechanism of the hydrogen-oxygen reaction i. the third explosion limit. *Proceedings of the Royal Society of London. Series A. Mathematical and Physical Sciences*, *185*(1003), 353–369. https://doi.org/10.1098/rspa.1946.0023

Zeng, Z., Dlugogorski, B. Z., Oluwoye, I., & Altarawneh, M. (2021). Combustion chemistry of COS and occurrence of intersystem crossing. *Fuel*, *283*, 119257. https://doi.org/10.1016/j.fuel.2020.119257